

## Perturbative and nonperturbative parts of eigenstates and local spectral density of states: The Wigner-band random-matrix model

Wen-ge Wang

*Department of Physics, South-east University, Nanjing 210096, China;*

*International Center for the Study of Dynamical Systems, 22100 Como, Italy;*

*Department of Physics and Centre for Nonlinear Studies, Hong Kong Baptist University, Hong Kong, China*

(Received 16 January 1998; revised manuscript received 22 July 1999)

The Wigner-band random-matrix model is studied by making use of a generalization of Brillouin-Wigner perturbation theory. Energy eigenfunctions are shown to be divided into perturbative and nonperturbative parts. Several perturbation strengths predicted by the perturbation theory are found to play important roles in the variation of the shape of the local spectral density of states with perturbation strength.

PACS number(s): 05.45.-a

The average shape of energy eigenfunctions (EF's), characterizing the spreading of perturbed eigenstates over unperturbed eigenstates, is of importance in a wide range of physical fields, from nuclear physics to condensed-matter physics (see, e.g., [1–6]). Recently, another important quantity, the so-called local spectral density of states (LDOS), has also attracted lots of attention (see, e.g., [5–9]). This quantity gives information about the “decay” of a specific unperturbed state into other states due to interaction. In particular, the width of LDOS defines the effective “lifetime” of the unperturbed state. Numerically, it is already known that for Hamiltonian matrices with band structure generally both the average shape of EF's and that of LDOS can be divided into two parts: central parts and tails with exponential (or faster) decay. However, an analytical definition for such a division has not been achieved yet. A possible clue for this problem comes from a generalization of the Brillouin-Wigner perturbation theory (GBWPT) introduced in Ref. [10] for studying long tails of EF's, which tells that analytically EF's can be divided into perturbative and nonperturbative parts with perturbative parts expanded in a convergent perturbation expansion. The relationship between central parts and nonperturbative parts of EF's was not studied in Ref. [10], but it is quite important as well.

The so-called Wigner-band random-matrix (WBRM) model was introduced by Wigner more than 40 years ago [11] for the description of complex quantum systems as nuclei. It is currently under close investigation (see, e.g., [12–17]) since it is believed to provide an adequate description also for some other complex systems, e.g., the Ce atom [5], and as well as for dynamical conservative systems possessing chaotic classical limit. Having been studied extensively both analytically and numerically, many of the properties of the WBRM are already known clearly, especially, analytical techniques for studying the LDOS of the WBRM have been developed quite well [7]. However, there are still some properties of the model which have not been studied, e.g., the division of EF's into perturbative and nonperturbative parts. It is such properties of the model that we are to study in this paper by making use of the GBWPT.

The Hamiltonian matrix of the WBRM model studied in this paper is chosen of the form  $H_{ij} = (H^0 + \lambda V)_{ij} = E_i^0 \delta_{ij}$

$+ \lambda v_{ij}$ , where  $E_i^0 = i$  ( $i = 1, \dots, N$ ) are eigenenergies of the eigenstates of  $H^0$  labeled by  $|i\rangle$  and  $\lambda$  is for adjusting the perturbation strength. Off-diagonal matrix elements  $v_{ij} = v_{ji}$  are random numbers with Gaussian distribution for  $1 \leq |i-j| \leq b$  ( $\langle v_{ij} \rangle = 0$  and  $\langle v_{ij}^2 \rangle = 1$ ) and are zero otherwise. Here  $b$  is the bandwidth of the Hamiltonian matrix and  $N$  is its dimension. Eigenstates of  $H$ , labeled by  $|\alpha\rangle$ , are also ordered in energy,  $H|\alpha\rangle = E_\alpha|\alpha\rangle$ .

Before discussing properties of the WBRM, let us first cite two results of the GBWPT in Ref. [10]. The first one is that, an eigenstate  $|\alpha\rangle$  can be divided into a nonperturbative (NPT) part  $|t\rangle \equiv P|\alpha\rangle$  and a perturbative (PT) part  $|f\rangle \equiv Q|\alpha\rangle$  by two projection operators  $P = \sum_{i=p_1}^{p_2} |i\rangle\langle i|$  and  $Q = 1 - P$ , where  $p_1$  and  $p_2$  are determined by two requirements: (i)  $(p_2 - p_1)$  has the smallest value, (ii)

$$\lim_{n \rightarrow \infty} \langle \alpha | (T^\dagger)^n T^n | \alpha \rangle = 0, \quad (1)$$

where  $T = [1/(E_\alpha - H^0)] Q \lambda V$ . (Subscripts  $\alpha$  for the operators  $P$  and  $Q$ , etc., are omitted for brevity.) The PT part  $|f\rangle$  can be expanded in a convergent perturbation expansion by making use of the NPT part  $|t\rangle$  even when perturbation is strong. The second result is that, defining the size of the NPT part  $|t\rangle$  as  $N_p \equiv p_2 - p_1 + 1$ , the perturbation strength at which  $N_p = b$ , denoted by  $\lambda_b$ , is of importance since the structure of the perturbation expansion of  $|f\rangle$  for the case of  $N_p \geq b$  is different from that for  $N_p < b$ . Another perturbation strength of interest is the smallest  $\lambda$  for  $N_p = 2$ , labeled by  $\lambda_f$ , which indicates the beginning of the invalidity of the ordinary Brillouin-Wigner perturbation theory.

Introducing an operator  $U \equiv QV[1/(E_\alpha - H^0)]Q$  and its eigenfunctions  $U|v\rangle = u_v|v\rangle$ , one can show that the condition (1) is equivalent to the requirement that all the values of  $|\lambda u_v|$  are less than one. Then, using the perturbation expansion of the PT part of  $|\alpha\rangle$  and an expansion  $Q\lambda V|t\rangle = \sum_v h_v|v\rangle$ , one can show that each component  $C_{\alpha j} = \langle j|\alpha\rangle$  with  $j \in [p_1 - (m+1)b, p_1 - mb)$  or  $(p_2 + mb, p_2 + (m+1)b]$ , where  $m \geq 0$ , can be expressed as

$$C_{\alpha j} = \frac{1}{E_\alpha - E_j^0} \sum_v \left[ \frac{h_v}{1 - \lambda u_v} \langle j|v\rangle \right] (\lambda u_v)^m. \quad (2)$$

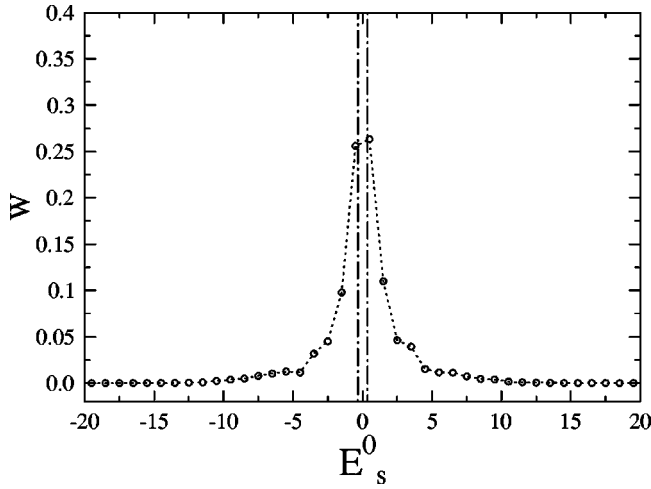


FIG. 1. The average shape of EF's in the middle energy region for  $\lambda=0.6$ ,  $b=10$ , and  $N=300$ . The vertical dashed-dot lines indicate positions of the averaged boundary  $p_1^a$  and  $p_2^a$  of the NPT parts of the EF's.

Since  $|\lambda u_\nu| < 1$  for all  $\nu$ , the behavior of the long tails of EF's of the WBRM is more or less like exponential decay. In fact, from the viewpoint of the GBWPT, the proof and arguments given in Ref. [5] for exponential-like behaviors of long tails of the LDOS of the WBRM are still valid when perturbation is strong. Equation (2) shows that the decaying speed of  $|C_{\alpha j}|$  for  $m=0$  should be slower than that for  $m > 0$ . The two regions  $(p_2, p_2+b]$  and  $[p_1-b, p_1)$  will be called the *slope* regions of the eigenstate  $|\alpha\rangle$ .

Now let us study the division of EF's into perturbative

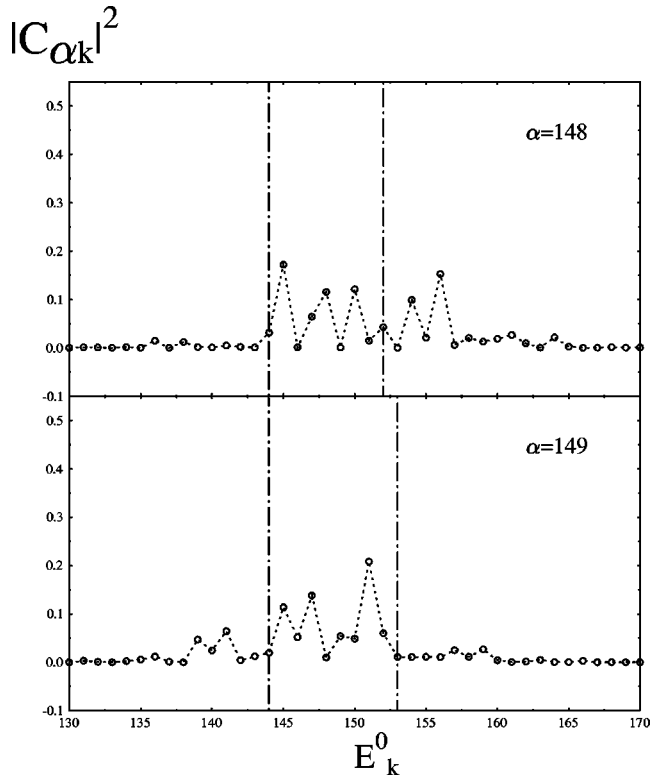


FIG. 2. Values of  $|C_{\alpha k}|^2$  (circles) for two states  $|\alpha\rangle$  when  $\lambda=1.4$ . Vertical dashed-dot lines indicate positions of the boundaries  $p_1$  and  $p_2$  of the NPT parts of the states.

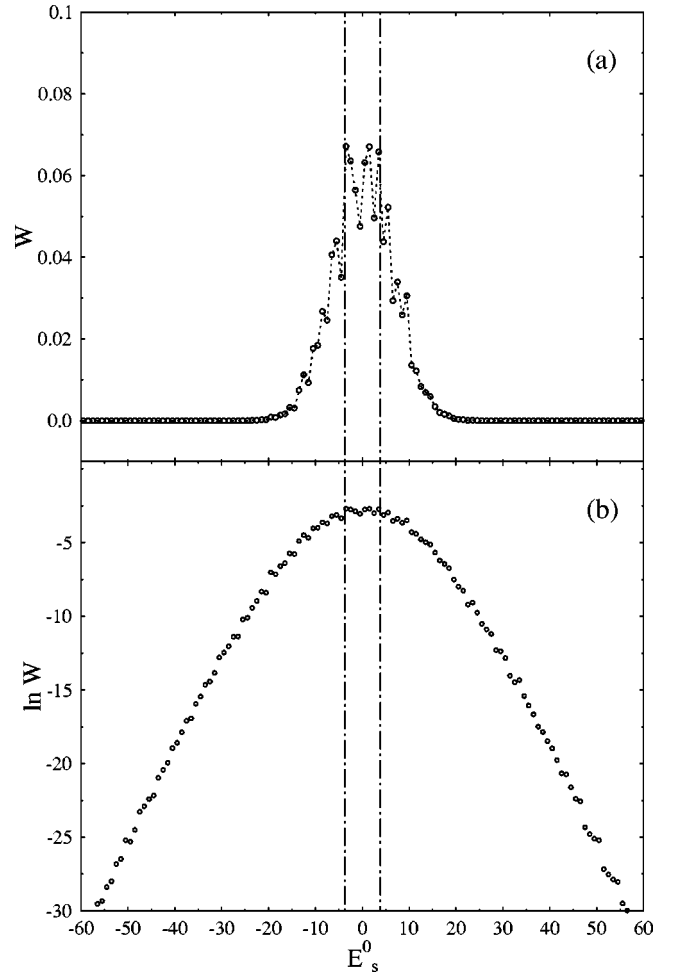


FIG. 3. (a) Same as in Fig. 1 for  $\lambda=1.4$ . (b) Same as in (a) in logarithm scale.

(PT) and nonperturbative (NPT) parts numerically. For an EF of an  $H$  matrix obtained by numerical diagonalization, the boundary of its NPT part is calculated by finding the pair(s) of  $(p_1, p_2)$  with the smallest  $N_p$  ensuring that condition (1) holds. In order to check the results thus obtained, eigenvalues of  $\lambda U$  are also calculated. The shape of an eigenstate  $|\alpha\rangle$  in the unperturbed states can be defined as  $W_\alpha(E^0) = \sum_k |C_{\alpha k}|^2 \delta(E^0 - E_k^0)$ , where  $C_{\alpha k} = \langle k | \alpha \rangle$ . In order to obtain the average shape of eigenstates, we express  $W_\alpha(E^0)$  with respect to  $E_\alpha$  before averaging. The average shape of eigenstates, denoted by  $W(E_s^0)$ , can also be divided into a NPT part and a PT part by the averaged boundary of the NPT parts of the states  $|\alpha\rangle$ , denoted by  $p_1^a \equiv \langle p_1 - E_\alpha \rangle$  and  $p_2^a \equiv \langle p_2 - E_\alpha \rangle$ , respectively. The average size of the NPT parts of eigenstates is  $\langle N_p \rangle \equiv \langle p_2 - p_1 + 1 \rangle$ .

The first numerical result we present is for the case of  $N=300$ ,  $b=10$ , and  $\lambda=0.6$ . This is a case for which  $N_p$  can be equal to both 1 and 2. The average shape of EF's for  $\alpha$  from 130 to 170 is given in Fig. 1 with the boundaries  $p_1^a$  and  $p_2^a$  indicated by vertical dashed-dot lines. Then, we increase the value of  $\lambda$  to 1.4. For this  $\lambda$ ,  $N_p=b$  for some of the eigenstates, e.g.,  $N_p=9,10$  for  $\alpha=148,149$ , respectively. Individual EF's for the two  $|\alpha\rangle$  are given in Fig. 2 with their boundaries of the NPT parts. The average shape of EF's in the middle energy region for  $\lambda=1.4$  is presented in Fig. 3(a),

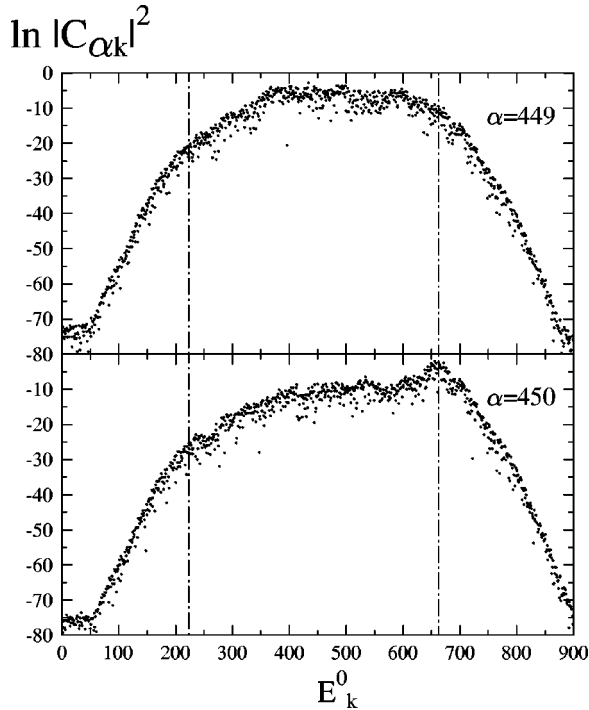


FIG. 4. Same as in Fig. 2 for  $\lambda = 30.0$ ,  $b = 10$ , and  $N = 900$  in logarithm scale.

the main body of which lies obviously in the averaged NPT region. Figure 3(a) also shows why the two regions  $[p_1^a - b, p_1^a]$  and  $(p_2^a, p_2^a + b]$  are called “slope” regions. Figure 3(b) shows that, as predicted above, the decaying speed of the averaged EF’s in the two slope regions is obviously slower than that in the long-tail regions.

A feature of the WBRM model is that in some regimes of the parameter there would appear the so-called localization in the energy shell [12]. Behaviors of EF’s in their NPT regions in these regimes of the parameter are different from that shown in Fig. 2. For example, as shown in Fig. 4, when

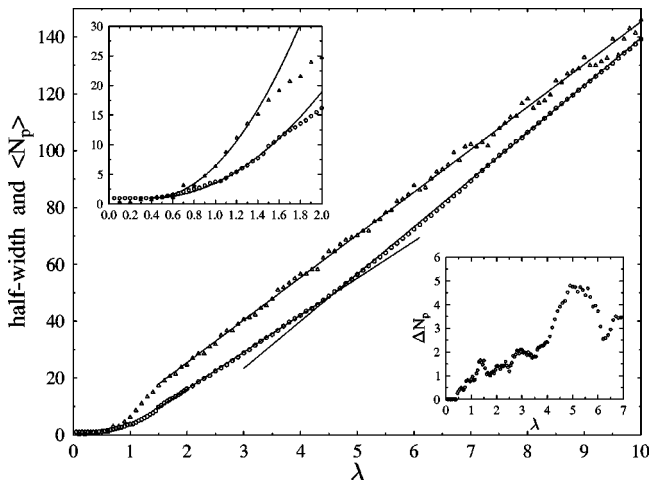


FIG. 5. Circles show the values of  $\langle N_p \rangle$  and the triangles show the half-width of the LDOS ( $N = 500, b = 10$ ). The three solid straight lines are fitting lines. The upper-left inset shows the fitting curves of the quadratic form for  $\langle N_p \rangle$  and for the half-width of the LDOS, respectively, for  $\lambda$  from 0.4 to 1.5. The lower-right inset shows the values of  $\Delta N_p$  (circles).

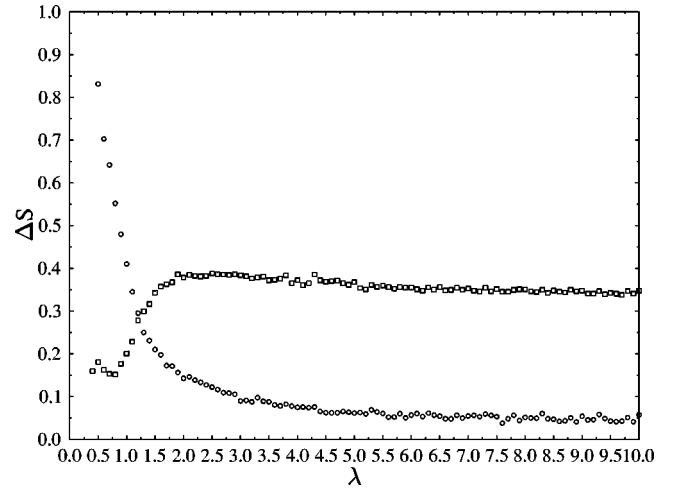


FIG. 6. Variation of  $\Delta S_{sc}$  (circles) and  $\Delta S_{BW}$  (squares) with  $\lambda$  ( $N = 500, b = 10$ ).

$\lambda = 30$ ,  $b = 10$ , and  $N = 900$ , the main bodies of the EF’s occupy only part of their NPT regions between  $p_1$  and  $p_2$ . This property of the EF’s could explain the phenomenon of localization in the energy shell. In our opinion, the localization is in fact localization of EF’s in their NPT regions. Figure 4 also shows that although many components of the NPT parts of the EF’s are quite small, their decaying speed is obviously slower than that in the PT parts of the EF’s. The average shape of the EF’s in this case has been found showing similar features as in Fig. 3 with respect to the NPT regimes.

In order to have a clear picture for the variation of the average size  $\langle N_p \rangle$  of NPT parts of EF’s with  $\lambda$ , we plot it in Fig. 5 by circles. Numerically we have found that  $\lambda_{f \min}$ , the smallest  $\lambda_f$ , is about 0.4 and  $\langle \lambda_b \rangle \approx 1.5$ . Figure 5 shows that  $\langle N_p \rangle$  has four types of behavior separated by three values of  $\lambda$ , namely,  $\lambda_{f \min}$ ,  $\langle \lambda_b \rangle$ , and  $\lambda_s \approx 4.5$ . When  $\lambda < \lambda_{f \min}$ ,  $\langle N_p \rangle = 0$ . In the region of  $(\lambda_{f \min}, \langle \lambda_b \rangle)$ , the value of  $\langle N_p \rangle$  has a quadratic dependence on  $\lambda$  (upper-left inset). When  $\lambda > \langle \lambda_b \rangle$ , the dependence of  $\langle N_p \rangle$  on  $\lambda$  becomes linear, but the slope for  $\lambda < \lambda_s$  is different from that for  $\lambda > \lambda_s$ . The variance of  $N_p$ , denoted by  $\Delta N_p$ , is small compared with  $N_p$  as shown in the lower-right inset of Fig. 5 (circles).

The local spectral density of states (LDOS) for an unperturbed state  $|k\rangle$  is defined as  $\rho_L^k(E) = \sum_\alpha |C_{\alpha k}|^2 \delta(E - E_\alpha)$ . The average shape of the LDOS, denoted by  $\rho_L(E_s)$  (subscript  $s$  will be omitted), can be obtained in a way similar to that for the EF’s discussed above, except that  $\rho_L^k(E)$  are expressed as functions of  $(E - E_k^0)$  before averaging. Properties of the LDOS of the WBRM have already been studied well (see, e.g., [5, 12, 14]), especially, the corresponding analytical techniques have already been developed well [7]. The reason for us to pay some attention to it in this paper is that the role of  $\lambda_b$  and  $\lambda_s$  has not been discussed in previous work.

Let us first study the transition of the average shape of the LDOS from the Breit-Wigner form to the semicircle form. For this we make use of two quantities  $\Delta S_{BW} = \int |\rho_L(E) - \rho_{BW}(E)| dE$  and  $\Delta S_{sc} = \int |\rho_L(E) - \rho_{sc}(E)| dE$ , which measure the deviation of the LDOS  $\rho_L(E)$  from its best fitting Breit-Wigner form and from the semicircle form, respectively,

$$\rho_{\text{BW}}(E) = \frac{\Gamma/2\pi}{E^2 + \Gamma^2/4}, \quad \rho_{\text{sc}}(E) = \frac{2}{\pi R_0^2} \sqrt{R_0^2 - E^2}, \quad (3)$$

where  $R_0 = \lambda \sqrt{8b}$ . Variation of the two quantities  $\Delta S_{\text{BW}}$  (squares) and  $\Delta S_{\text{sc}}$  (circles) with  $\lambda$  are given in Fig. 6. For  $\lambda$  a little larger than  $\lambda_{f \min}$ , as is well known, the LDOS  $\rho_L(E)$  is close to the Breit-Wigner form and  $\Delta S_{\text{BW}}$  is small. When  $\lambda$  reaches  $\langle \lambda_b \rangle \approx 1.5$ , the LDOS  $\rho_L(E)$  is absolutely different from the Breit-Wigner form, while it becomes close to the semicircle form. When  $\lambda$  is larger than  $\lambda_s \approx 4.5$ , the value of  $\Delta S_{\text{sc}}$  becomes quite small, indicating that the LDOS is already quite close to the semicircle form. Since the semicircle form  $\rho_{\text{sc}}(E)$  obeys a scaling law under  $E \rightarrow E/\lambda$ ,  $\rho_{\text{sc}} \rightarrow \lambda \rho_{\text{sc}}$ , and  $R_0 \rightarrow R_0/\lambda$ , when the LDOS  $\rho_L(E)$  is close to the semi-circle form, it should obey an approximate scaling law. Therefore, the perturbation strength  $\lambda_s$  can be regarded as characterizing the beginning for the LDOS to obey a good approximate scaling law. Second, let us study the half-width

of the average shape of LDOS, the variation of which is given in Fig. 5 by triangles. We see that the well-known quadratic dependence and linear dependence of the half-width on perturbation strength is separated by the perturbation strength  $\langle \lambda_b \rangle$ .

In conclusion, in this paper numerically it is shown that the central part of the average shape of EF's is composed of its nonperturbative (NPT) part and the slope region of its perturbative (PT) part predicted by the GBWPT. Three perturbation strengths related to properties of the size of NPT parts of EF's, namely,  $\lambda_f$ ,  $\lambda_b$ , and  $\lambda_s$ , have been found also to play important roles in the variation of the shape of the LDOS.

This work was partly supported by the National Basic Research Project "Nonlinear Science," China, the Natural Science Foundation of China, Grants from the Hong Kong Research Grant Council (RGC), and a Hong Kong Baptist University Faculty Research Grant (FRG).

- 
- [1] B. Georgeot and D.L. Shepelyansky, Phys. Rev. Lett. **79**, 4365 (1997).  
 [2] Y.V. Fyodorov and A.D. Mirlin, Phys. Rev. B **52**, R11 580 (1995); K. Frahm and A. Müller-Groeling, Europhys. Lett. **32**, 385 (1995).  
 [3] V.V. Flambaum, F.M. Izrailev, and G. Casati, Phys. Rev. E **54**, 2136 (1996).  
 [4] V.V. Flambaum and F.M. Izrailev, Phys. Rev. E **55**, R13 (1997); **56**, 5144 (1997).  
 [5] V.V. Flambaum, A.A. Gribakina, G.F. Gribakin, and M.G. Kozlov, Phys. Rev. A **50**, 267 (1994).  
 [6] V. Zelevinsky, B.A. Brown, M. Horoi, and N. Frazier, Phys. Rep. **276**, 85 (1996).  
 [7] Y.V. Fyodorov, O.A. Chubykalo, F.M. Izrailev, and G. Casati, Phys. Rev. Lett. **76**, 1603 (1996).  
 [8] Ph. Jacquod, D.L. Shepelyansky, and O.P. Sushkov, Phys. Rev. Lett. **78**, 923 (1997).  
 [9] A.D. Mirlin and Y.V. Fyodorov, e-print cond-mat/97002120.  
 [10] Wen-ge Wang, F.M. Izrailev, and G. Casati, Phys. Rev. E **57**, 32 (1988).  
 [11] E. Wigner, Ann. Math. **62**, 548 (1955); **65**, 203 (1957).  
 [12] G. Casati, B.V. Chirikov, I. Guarneri, and F.M. Izrailev, Phys. Lett. A **223**, 430 (1996).  
 [13] M. Feingold, D.M. Leitner, and O. Piro, Phys. Rev. A **39**, 6507 (1989); M. Feingold, D. Leitner, and M. Wilkinson, Phys. Rev. Lett. **66**, 986 (1991); J. Phys. A **24**, 1751 (1991); D.M. Leitner and M. Feingold, *ibid.* **26**, 7367 (1993).  
 [14] G. Casati, B.V. Chirikov, I. Guarneri, and F.M. Izrailev, Phys. Rev. E **48**, R1613 (1993).  
 [15] A. Gioletta, M. Feingold, F.M. Izrailev, and L. Molinari, Phys. Rev. Lett. **70**, 2936 (1993).  
 [16] T. Prosen and M. Robnik, J. Phys. A **26**, 1105 (1993).  
 [17] T. Guhr, A. Müller-Groeling, and H.A. Weidenmüller, Phys. Rep. **299**, 189 (1998).